Quantum Electronics **33** (7) 628 – 632 (2003)

PACS numbers: 42.79. Hp; 42.68. Mj; 42.62. Fi
DOI: 10.1070/QE2003v033n07ABEH002469

Atomic opto-spintron correlator based on selective specular reflection

V.I. Balykin, V.S. Letokhov

***Abstract*. The possibility of the development of a fast, energy-efficient optical correlator based on the optical orientation and reorientation of nuclear spins in atoms is studied.**

Keywords: *optical correlator, optical nonlinearity, spin.*

1. Introduction

The use of optical radiation as an information carrier offers a number of potential advantages over electrical signals. These advantages, related to the physical properties of light fluxes, are as follows: (i) light fluxes do not interact with each other in a linear optical medium, even when crossed, which allows a fast parallel processing of large data arrays; (ii) light fluxes can be localised within a region of size lower than 1 μm in the transverse direction to the light beam; when ultrashort pulses are used, the light fluxes can be also localised within micron region in the longitudinal direction; (iii) the transfer rate of an optical signal exceeds that of an electrical signal; and (iv) the use of optical radiation as an information carrier excludes the necessity of repeated conversion of the electric energy to light energy and vice versa. These properties of laser radiation eliminate the restrictions on the time response and parallel data processing inherent in electric signals.

The most specific property of optical radiation as an information carrier is that it provides two-dimensional, and in the case of ultrashort pulses, even three-dimensional data transfer and processing. Two-dimensional data transfer and processing is possible due to a small wavelength of light (less than 1 μm in the visible range), which allows one to use laser radiation for producing images of size ~ 1 μm. This in turn provides the transfer of up to 10^{10} data bits in an optical beam of diameter 3 cm.

The potential advantages of optical radiation as an information carrier have not been realised so far because of the absence of the efficient methods for coupling information into optical radiation and decoupling it out. In most studies devoted to optical data processing, the temporal modulation of a single laser beam was considered, which excludes the main advantage of optical radiation - its two-dimensionality and, therefore, the possibility of parallel optical data processing.

Parallel optical data processing can be performed with the help of an optical correlator (OC), which is intended for signal processing in receiver – transmitters of the correlation type. The operation of an OC is based on a comparison of the pattern image to be recognised with a reference image. If the image contains the pattern of interest to us, an auto-correlation signal appears, indicating the presence of the pattern being recognised. OCs can be used for rapid comparison of an input image with a huge image library, i.e., for parallel two-dimensional optical data processing. Fast OCs are most suitable for applications in medical diagnostics, meteorology, criminology, etc. However, their potential has not been realised so far due to the absence of appropriate materials and the physical mechanism that would provide rapid optical data writing and reading.

At present, several particular OC schemes have been proposed. The most efficient schemes are based on the three- and four-wave mixing of optical waves in nonlinear optical materials [1] such as photorefractive crystals and atomic vapours. Photorefractive-crystal OCs have been demonstrated experimentally. However, because their time response was only 0.03 s, the real-time image processing was performed too slowly. Another important disadvantage of such an OC is a high optical energy required for switching the correlator over from one stable state to another.

An OC based on atomic medium with a high optical nonlinearity was proposed in paper [2] and realised experimentally in paper [3]. This correlator had much better temporal and energy parameters. Its time response can achieve $\sim 10^{-8}$ s (the lifetime of an excited state of an atom) and the spatial resolution can be ~ 1 μm. Nevertheless, the use of optical nonlinearity in the OC assumes the employment of high-power radiation in atomic media as well.

In this paper, we further develop an OC based on atomic media. The correlator proposed in our paper differs from other OCs by the use of selective specular reflection of light from an atomic gas.

2. Selective specular reflection of light from an atomic gas

Specular reflection of light from an atomic gas at a resonance frequency was discovered by Wood [4]. The essence of this phenomenon is as follows. Resonance

V.I. Balykin, V.S. Letokhov Institute of Spectroscopy, Russian Academy of Sciences, 142190 Troitsk, Moscow region;
e-mail: balykin@isan.troitsk.ru

Received 23 January 2003
Kvantovaya Elektronika **33** (7) 628 – 632 (2003)
Translated by M.N. Sapozhnikov

radiation incident on a rarefied atomic medium is isotropically scattered in the medium. As the gas pressure increases, the average distance between atoms decreases, and when the distance becomes smaller than the wavelength of the incident light, interference between spherical waves emitted by individual atoms results in the appearance of a plane wave propagating in the specular reflection direction. Two conditions should be fulfilled for specular coherent reflection to occur: (i) for a plane wave to be formed, the absorption coefficient should exceed the absolute value of the wave vector of incident radiation; and (ii) to eliminate the Doppler effect, the mean free path of an atom should be smaller than the radiation wavelength. Specular reflection occurs in experiments, as a rule, from a flat interface between a dielectric and atomic gas.

The type of selective reflection strongly depends on the atomic gas pressure. At high pressure, when the collision broadening γ_c of an optical transition is larger than the inhomogeneous (Doppler) broadening $\Delta\omega_D$, specular reflection is well described by the classical dispersion theory [5, 6]. At relatively low gas pressures, when $\gamma_c < \Delta\omega_D$, collisions of atoms with the dielectric surface limiting the gas volume introduce some specific features to the type of reflection [6, 7]. A low contrast of specular resonance reflection with respect to a nonselective background upon normal incidence of radiation on the dielectric-atomic gas interface restricts the application of this method in the case of normal incidence. At larger angles of incidence, total internal specular reflection occurs, which acquires at sufficiently high pressures a unique property – a high reflection coefficient, which can be both linear [4] and nonlinear [8]. The known application of this effect to stabilise the laser frequency was proposed even in 1970 [8].

The basic qualitative characteristics of specular reflection can be obtained by considering the reflection of a plane wave from the dielectric–atomic gas interface. Let us assume that the electric field

$$\boldsymbol{E}(\boldsymbol{r},t) = \boldsymbol{E}_0 \exp[\mathrm{i}(\boldsymbol{kr} - \omega t)] + \text{c.c.} \tag{1}$$

of a wave incident on the interface excites an oscillating electric dipole moment

$$\boldsymbol{P}(\boldsymbol{r},t) = \boldsymbol{P}_0 \exp[\mathrm{i}(\boldsymbol{kr} - \omega t)] + \text{c.c.} \tag{2}$$

in each atom of the gas.

In the case of the weak incident field, the dipole amplitude is proportional to the electric-field amplitude:

$$p = \alpha E, \tag{3}$$

where α is the dielectric susceptibility of the atom. The macroscopic polarisability in the atomic medium can be represented in the form

$$P = N\alpha E = \chi \exp[\mathrm{i}(\boldsymbol{kr} - \omega t)], \tag{4}$$

where $\chi = \alpha N$ is the dielectric susceptibility of the gas and N is the number of atoms (in 1 cm^3). The dielectric susceptibility of a real atom also depends on the angular momenta of its ground and excited states [9, 10]

$$\chi = \chi_{is} + \chi_{hfs}\boldsymbol{IJ} - \mathrm{i}\sum_{F,F'} \chi_{gt}(F,F')\boldsymbol{J}(F,F')X + \sum_{F,F'} \chi_{br}(F,F')Q, \tag{5}$$

where χ_{is} is the isotropic part of the dielectric susceptibility; χ_{hfs} is the part of the susceptibility depending on the hyperfine structure of the atomic level; $\chi_{gt}(F,F')$ is the gyrotropic part of the susceptibility responsible for circular dichroism of the atomic gas and optical rotation; $\chi_{br}(F,F')$ is the part of the susceptibility responsible for light-induced anisotropy in vapours; $\boldsymbol{J}$, $\boldsymbol{I}$, and F are the atomic orbital angular momentum, nuclear spin angular momentum, and total angular momentum of the atom; Q is the electric quadrupole moment of the atom; and the symbol X means vector multiplication by any vector to the right.

It was shown in paper [6] that for $\gamma_c > \Delta\omega_D$, all the relations in the optics of transparent media, obtained from Maxwell's equations and boundary conditions, can be formally applied in the optics of absorbing media after the replacement of the real dielectric constant ε (or dielectric susceptibility χ) by the complex quantity $\varepsilon^* = \varepsilon' - \mathrm{i}\varepsilon''$. Then, the coefficients of reflection of light from the interface depend on the dielectric susceptibility and the angle of incidence φ on the interface as

$$R_\perp = \frac{(a - \cos\varphi)^2 + b^2}{(a + \cos\varphi)^2 + b^2}, \tag{6}$$

$$R_\parallel = \frac{[(a - \cos\varphi)^2 + b^2][(a - \sin\varphi\tan\varphi)^2 + b^2]}{[(a + \cos\varphi)^2 + b^2][(a + \sin\varphi\tan\varphi)^2 + b^2]}, \tag{7}$$

where $R_\perp$ and $R_\parallel$ are the reflection coefficients for the radiation components for which the electric-field vector lies in the plane of incidence or perpendicular to it, respectively; and the parameters a and b are defined by the expressions

$$2a^2 = \Big\{(1 + \chi' - \sin^2\varphi) + \big[(1 + \chi' - \sin^2\varphi)^2 + (\chi'')^2\big]^{1/2}\Big\}, \tag{8}$$

$$2b^2 = \Big\{-(1 + \chi' - \sin^2\varphi) + \big[(1 + \chi' - \sin^2\varphi)^2 + (\chi'')^2\big]^{1/2}\Big\}, \tag{9}$$

where χ' and χ'' are the real and imaginary parts of the dielectric susceptibility.

3. Atomic opto-spintron correlator

Consider the possibility of constructing an optical correlator based on specular reflection using different parts of the *atomic* dielectric susceptibility (5). Here, we call by the optical correlator its part where the physical process of information exchange occurs between a laser beam carrying the information and a probe beam reading the information. Such a correlator should naturally include the third component where information exchange takes place between the two beams. In our case, it is an *atomic gas with the nonzero spin moment* of the ground or excited state. The atomic medium can be conveniently described using the dielectric susceptibility χ (5). The information exchange

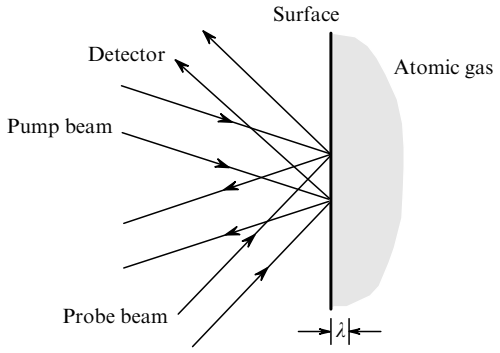

Figure 1. Scheme of the atomic opto-spintron correlator based on the nonlinear susceptibility of an atomic medium and selective specular reflection.

occurs upon selective specular reflection of both laser beams, as shown schematically in Fig. 1. We call such a correlator the atomic opto-spintron correlator (AOC).

3.1 Atomic correlator based on the isotropic dielectric susceptibility χ_{is}

The possibility of using nonlinear optical media in optical computers has long attracted attention of researchers. Eremeeva and co-workers [11] proposed a concrete scheme of nonlinear three-wave mixing to perform the convolution operation and correlation analysis. Yariv [12] proposed to use three-wave mixing for producing real-time holograms.

Three-wave mixing schemes are inherently restricted over the spatial frequency band due to the necessity of having phase matching. Another drawback of these schemes is the necessity of using multifrequency radiation. Four-wave mixing is a nonlinear physical process free of these problems [13]. Nonlinear effects appearing upon selective reflection from the dielectric-atomic gas interface were considered in paper [14] where a change in the reflection of a probe field in the presence of a strong field was calculated in terms of the effective dielectric susceptibility. It was shown that the isotropic part of the dielectric susceptibility at the probe-field frequency depends on the strong-field intensity as

$$\chi_{is} = \chi_{is}^{0} + \Omega_R^2 \chi_{is}', \tag{10}$$

where χ_{is}^{0} is the susceptibility of atoms in the absence of a strong field; χ_{is}' is the coefficient characterising the nonlinearity of the optical medium, independent of the Rabi frequency of the strong field; and Ω_R is the Rabi frequency of the strong field.

Although an AOC based on specular reflection and optical nonlinearity of an atomic medium, as well as an OC based on absorption in an atomic gas [13], requires an appreciable power per pixel, its substantial advantage is an extremely small size of a pixel, equal to the radiation wavelength, because the 'thickness' of the active zone of the correlator is smaller than the wavelength of light, i.e., the correlator is not a bulk correlator (as all known correlators) but a plane one.

3.2 Atomic correlator based on optical pumping (using the dielectric susceptibility χ_{hfs})

If the ground state of atoms is split (for example, due to the hyperfine splitting), then the dielectric susceptibility is a function of the populations of the corresponding sublevels of the ground state. The ground state of alkali-metal atoms is split due to the hyperfine interaction into two sublevels – $F_1 = |\boldsymbol{J} + \boldsymbol{I}|$ and $F_2 = |\boldsymbol{J} - \boldsymbol{I}|$. For example, $F_2 = 2$ and $F_1 = 1$ for a sodium atom. When the sublevels F_1 and F_2 are populated according to their statistical weights, then $\langle \boldsymbol{IJ} \rangle = 0$ and the corresponding averaged hyperfine part of the susceptibility of the atomic medium, as follows from (5), is also zero. When all the atoms are on the upper sublevel $F = 2$, then $\langle \boldsymbol{IJ} \rangle = 3/4$ and the susceptibility is maximum at the transition frequency with $F = 2$. If all the atoms are on the lower sublevel $F = 1$, then $\langle \boldsymbol{IJ} \rangle = -5/4$ and the hyperfine part of the susceptibility is maximum at the transition with $F = 1$.

Fig. 2 shows the energy level diagram for gas atoms in an optically pumped AOC. The strong field is resonant with the $F = 2 \rightarrow 3P_{1/2}$ transition and the probe field is resonant with the $F = 1 \rightarrow P_{1/2}$ transition. The basic energy and temporal parameters of the AOC can be easily estimated. The laser radiation intensity required to produce a noticeable redistribution of populations between two sublevels can be estimated from the energy balance condition

$$I = \frac{\hbar \omega N l}{T \rho}, \tag{11}$$

where $\rho = \Gamma_1 \tau = \Gamma_1/(\Gamma_1 + \Gamma_2)$; $1/T$ is the rate of relaxation of populations between the sublevels F_1 and F_2; $\tau = (\Gamma_1 + \Gamma_2)^{-1}$ is the spontaneous lifetime of the excited level; Γ_1 and Γ_2 are the rates of decay of the excited level to the sublevels F_1 and F_2, respectively; and l is the length of the interaction region. In the regime of total internal reflection, the characteristic length of the interaction region and its minimal transverse size (minimal size of a pixel) is of the order of the wavelength of light, i.e., the volume of a pixel is $\sim \lambda^3$. Expression (11) gives the estimate of the maximum number of photons required to pump optically one pixel:

$$n_{ph} = \frac{1}{\rho} \frac{N \lambda^3}{T}. \tag{12}$$

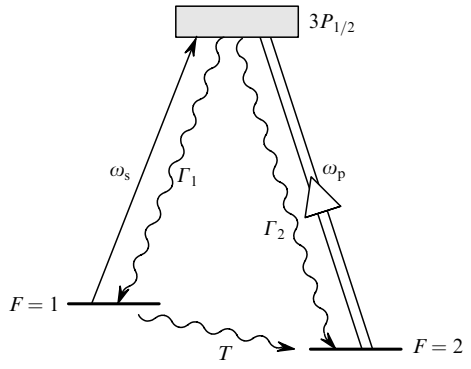

Figure 2. Energy level diagram for the optically pumped atomic opto-spintron correlator.

The time T of relaxation between the hyperfine-structure sublevels determines the time response of the AOC, which depends, in the geometry under study, on collisions of gas atoms with the dielectric surface. During collisions, the atoms pass to the thermal equilibrium with the surface, and the equilibrium population is established between the sublevels F_1 and F_2. The corresponding characteristic time is equal to the time $T_{\rm fl}$ of flight of an atom at the average velocity $\bar{v}_{\rm a}$ through the region of interaction with radiation, which is of the order of λ, i.e., the relaxation time

$$T_{\rm rel} = T_{\rm fl} = \frac{\lambda}{\bar{v}_{\rm a}} = 2 \times 10^{-9}\ {\rm c}. \tag{13}$$

Because the relaxation time $T_{\rm rel}$ can be shorter than the spontaneous decay time $\tau_{\rm sp}$ of the excited level, the number $n_{\rm ph}$ of photons in (12) should be estimated by using $\tau_{\rm sp}$ instead of T. The maximum density of atoms is determined as the density providing the maximum reflectivity. An increase in the reflection coefficient with increasing gas pressure is limited by the increase in the probability of triple collisions. The maximum pressure of atomic vapours, determined by this effect, is of the order of 10^2 Torr, corresponding to $N = 1.8 \times 10^{18}$ cm^{-3}. Then, the maximum laser radiation power required for one pixel $P_{\max} = (\hbar\omega N\lambda^3)(\rho\tau_{\rm sp})^{-1} = 2 \times 10^{-5}$ W and the switching energy per pixel is $W = P_{\max}\tau_{\rm sp} = 4 \times 10^{-14}$ J, corresponding to $n_{\rm ph} = W/\hbar \simeq 10^5$ photon pixel^{-1}. In this case, the time response of the correlator is $\sim 10^{-8}$ s.

The requirements to the energy parameters of the AOC can be substantially alleviated if the number of atoms in a pixel is restricted by $\sim$100, which is, nevertheless, provides a sufficiently high reflection coefficient. Then, the laser radiation power per pixel is $P_{\rm las} = 6 \times 10^{-9}$ W, the energy is $W = 6 \times 10^{-17}$ J, and the number of photons is $n_{\rm ph} = 10^2$ photon pixel^{-1}.

3.3 Atomic correlator based on a gyrotropic atomic medium

It is well known that the optical properties of weakly absorbing crystalline media are described by the complex tensor of the dielectric constant ε_{kl} (or the complex dielectric susceptibility χ_{kl}), which characterises the dependence of the optical properties of crystals on the direction of light propagation and its polarisation. In vapours of atoms with the nonzero angular momentum, a similar anisotropy appears in an external magnetic field. The anisotropic properties of atomic vapours are described by the dielectric susceptibility $\chi_{\rm gt}$ and $\chi_{\rm br}$ from (5). The susceptibility $\chi_{\rm gt}$ describes the gyrotropic properties of a medium and $\chi_{\rm br}$ describes its birefringence.

The gyrotropy of a medium is manifested in the phenomenon of circular dichroism and Faraday optical rotation. The physics of these phenomena in atomic vapours can be easily explained by analysing the interaction of a two-level atom with a quasi-equilibrium monochromatic field with the frequency ω. Consider an atomic medium placed in a magnetic field of strength B and excited by a linearly polarised light with the wave vector k directed along the magnetic field. The induced dipole moment of an atom has the component in phase with the magnetic field, to which the real part n_ω of the dielectric susceptibility corresponds, and the component shifted in phase by 90°, to which the imaginary part κ_ω of the susceptibility (absorption of light) corresponds. The magnetic field B splits the Zeeman sublevels of the excited state by $m_{\rm e}\mu B$, where $m_{\rm e} = \pm 1$ and μ is the magnetic moment of the atom. A linearly polarised light incident on the medium can be represented as a sum of two waves with polarisations σ^+ and σ^- and equal amplitudes coupling the ground state with two sublevels $m_{\rm e} = \pm 1$ of the excited state of the atom. These waves propagate in the atomic medium with different refractive indices n_+ and n_- and different absorption cross sections κ_+ and κ_-, and experience different phase shifts and attenuations. The phase shifts of the waves with polarisations σ^+ and σ^- lead to the rotation of the polarisation plane through the angle (Faraday rotation angle)

$$\beta = (\pi/\lambda)(n_+ - n_-)l. \tag{14}$$

For an atomic medium in a weak magnetic field ($\mu B < \Gamma$), the Faraday rotation angle is

$$\beta \approx (2\pi\kappa l)(\mu B/\Gamma), \tag{15}$$

i.e., it is determined by the product of the optical density $2\pi\kappa l$ by the Zeeman splitting in units of the homogeneous width $\mu B/\Gamma$. The Faraday effect in atomic vapours is four orders of magnitude larger than that in typical Faraday materials due to an extremely high sensitivity of atomic levels to a magnetic field.

The light fields with polarisations σ^+ and σ^- experience different absorption near the resonance, resulting in circular dichroism. The refraction and absorption of light lead to the elliptic polarisation of light transmitted through the atomic medium. The axial ratio of the polarisation ellipse is determined by the difference in absorption of the σ^+ and σ^- fields, and the Faraday angle is the angle between the initial polarisation vector and the major axis of the polarisation ellipse.

The AOC based on the gyrotropic susceptibility $\chi_{\rm gt}$ of an atomic medium and selective specular reflection can be implemented using the scheme shown in Fig. 3. A strong σ^+ polarised laser field (which can be spatially and temporarily modulated) prepares the atomic medium at

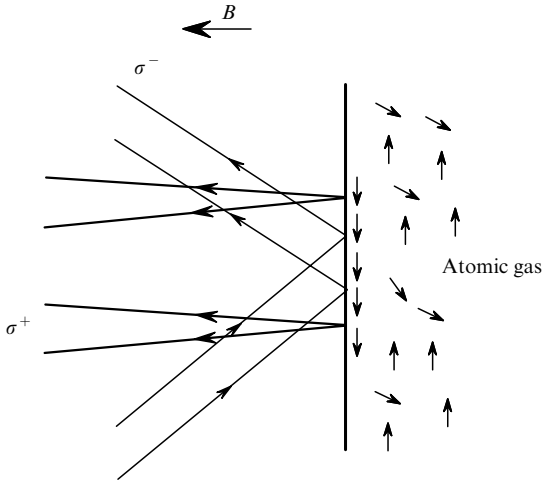

Figure 3. Atomic opto-spintron correlator based on the gyrotropic susceptibility of an atomic medium and selective specular reflection.

the interface with a nonzero Zeeman angular momentum $\langle J(F, F')\rangle$, resulting in circular dichroism. The selective resonance reflection of a probe field depends on the value of induced dichroism. The energy and temporal parameters of the AOC based on gyrotropic effects are comparable with those of optically pumped OCs.

It is well known that induced atomic orientation and polarisation can be both preserved and destroyed in collisions with the walls (depending on their material), which allows one to vary the time response of the AOC based on polarisation effects.

4. Conclusions

Note that the spatial resolution of the opto-spintron correlator considered above can be improved to achieve the submicron resolution. Such a high resolution can be obtained by localising a light field in the so-called near-field nanoprobes [15–17]. The methods for a sufficiently fast and highly sensitive manipulation of an optical nanoprobe have been realised [18]. Moreover, recently a trapezoid-configuration device was demonstrated [19] that provided a significant increase in the transmission of light through a nanoaperture of diameter $a_0 \approx 40 - 60$ nm. To use the near field in the region of the 2D scan with the area λ^2 of each nanoprobe of the array, the array of such nanoprobes should be used in the OC [20]. Then, the density of optical correlation elements can be increased by a factor of $(L/\lambda)^2 \simeq (\lambda/a_0)^2 \simeq (L/a_0)^2$, where L is the transverse size of the nanoprobe array with the total number of nanoprobes equal to $(L/\lambda)^2$. At the same time, the total time of data processing on the area L^2 will be determined only by the time of the 2D scan of the nanoprobe array in the region with the number of elements equal to $(a_0/\lambda)^2 \simeq 10^2 - 10^4$. Analysis of this possibility is beyond the scope of the AOC considered here. However, this possibility is quite real, especially in the context of the recent demonstration of the optically controlled spintron memory in *n*-doped InAs–GaAs quantum dots [21]. In this connection the development of 2D nanoprobe arrays based on quantum dots seems quite realistic.

Acknowledgements. This work was partially supported by the INTAS 'INFO 00-479' project and the Russian Foundation for Basic Research (Grant Nos 02-02-17014 and 02-16337a). The authors thank M. Ducloy and I. Bloch for useful discussions of the results.

References

1. White J., Yariv A. *Appl. Phys. Lett.*, **37**, 5 (1980).
2. Ai B., Glassner D.S., Knize R.J., Partanen J.P. *Appl. Phys. Lett.*, **64**, 851 (1994).
3. Biaggo I., Partanen J.P., Ai B., Knize R.J., Hellwarth R.W. *Nature*, **371**, 318 (1994).
4. Wood R.W. *Phil. Mag.*, **18**, 187 (1909).
5. Lauriston A.S., Welch H.L. *Can. J. Phys.*, **29**, 93 (1951).
6. Schuurmans M.F.H. *J. Physique*, **37**, 469 (1976).
7. Cojan J.L. *Ann. Physique* (Paris), **2**, 385 (1954).
8. Letokhov V.S. *Kratk. Soobshch. Fiz. FIAN*, **11**, 14 (1970).
9. Happer W., Mathur B.S. *Phys. Rev.*, **163**, 12 (1967).
10. Happer W. *Rev. Mod. Phys.*, **44**, 169 (1972).
11. Eremeeeva R.A., Kudryashov V.A., Matriev I.N., Usacheva T.G., Chekmenev A.I. *Kvantovaya Elektron.*, **5**, 1429 (1978) [*Sov. J. Quantum Electron.*, **8**, 818 (1978)].
12. Yariv A. *Appl. Phys. Lett.*, **28**, 89 (1976); *J. Opt. Soc. Am.*, **60**, 301 (1976).
13. Depper D.M., Yeung J.Au., Fekete D., Yariv A. *Opt. Lett.*, **3**, 7 (1978).
14. Schuller F., Nienhnis G., Ducloy M. *Phys. Rev. A*, **43**, 443 (1991).
15. Pohl D.W., Denk W., Lanz M. *Appl. Phys. Lett.*, **44**, 651 (1984); Lewis A., et al. *Ultramicroscopy*, **13**, 227 (1984); Fischer U.C. *J. Vac. Sci. Technol. B*, **3**, 386 (1985).
16. Betzig E., et al. *Science*, **251**, 1468 (1991); Betzig E., Trautman J.K. *Science*, **257**, 189 (1992).
17. Paesler M.A., Moyer P. *Near-Field Optics: Theory, Instrumentation, and Applications* (New York: John Wiley & Sons, 1996).
18. Serebryakov D.V., Cherkun A.P., Loginov B.A., Letokhov V.S. *Rev. Sci. Instr.*, **73**, 1795 (2002).
19. Naber A., Molenda D., Fischer U.C., Maas H.-J., Höppener C., Lu N., Fuchs H. *Phys. Rev. Lett.*, **89**, 210801 (2002).
20. Kim Y.-J., Suzuki K., Goto K. *Jpn. J. Appl. Phys.*, **40**, 1783 (2001).
21. Cortez S., Krebs O., Laurent S., Senes M., Marie X., Voisin P., Ferreira R., Bastard G., Gerard J.-M., Amand T. *Phys. Rev. Lett.*, **89**, 207401 (2002).